ACS APPLIED NANO MATERIALS

www.acsanm.org

Article

N-Succinyl Chitosan and Quaternary Chitosan Electrospun Nanofibers for Antiviral Filters against Enveloped Viruses

Khanyisile S. Dhlamini, Cyril T. Selepe, Bathabile Ramalapa, Krishna K. Govender, Lesego Tshweu,* and Suprakas Sinha Ray*

Cite This: https://doi.org/10.1021/acsanm.5c03567

Read Online

ACCESS | Metrics & More | Article Recommendations | Supporting Information

ABSTRACT: Globally, enveloped viruses have caused many fatalities, especially during outbreaks and pandemics. Developing antiviral filters that can reduce mortality rates caused by enveloped viruses is essential, particularly in preventing the spread of infectious diseases. In this study, two chitosan derivatives—*N*-succinyl chitosan (NSC) and *N*-(2-hydroxy)propyl-3-trimethylammonium chitosan chloride (HTCC)—were synthesized. For the first time, the antiviral activity of NSC against human immunodeficiency virus (HIV-1) was assessed. The two derivatives were further reduced to nanoscale through polyelectrolyte complexation to evaluate their combined antiviral activity for the first time. The nanoparticles (NPs) were incorporated into an interconnected network of ethyl cellulose nanofibers created via electrospinning to increase surface area. These nanofibers were used to develop an antiviral filter targeting enveloped viruses. They were characterized by their morphology, surface charge, pore size, and surface area—key factors influencing their filtration effectiveness. In vitro cytotoxicity tests indicated that the filters were nontoxic to TZM-bl cells, supporting their safety. Neutralization assays demonstrated that the filters could inhibit over 70% of HIV-1 infections within 40 s. Reusability studies revealed that the filters could be used up to three times with inhibition rates exceeding 90%. The findings show that these nanoparticles and nanofiber filters are effective and safe for antiviral applications.

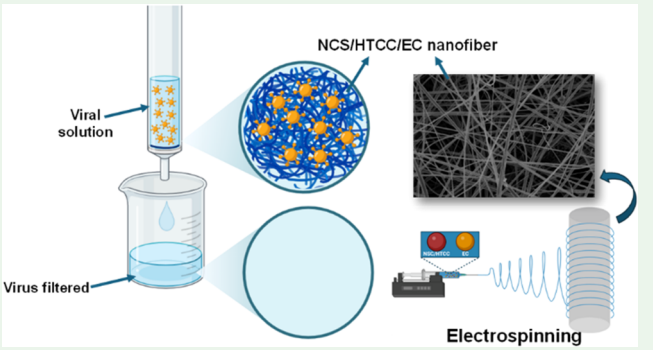

KEYWORDS: *enveloped viruses, nanofibers, ethylcellulose, HTCC, NSC, antiviral activity, antiviral filter*

1. INTRODUCTION

Globally, enveloped viruses have caused numerous fatalities, especially during outbreaks and pandemics, posing significant threats to human health.[1] These viruses contribute to disease transmission, leading to widespread illness and death, as many populations lack immunity to new viral strains.[2] One of the deadliest pandemics in history was caused by the Spanish Flu, which killed over 50 million people and infected more than 500 million worldwide in 1918.[3] Since the start of the human immunodeficiency virus (HIV) pandemic, 40 million people have died from HIV-related illnesses globally. It is also estimated that HIV is responsible for more than 680,000 deaths annually.[4] As of August 27, 2023, over 770 million confirmed cases of coronavirus disease (COVID-19) have been reported, with more than 6.9 million deaths.[5] Developing antiviral filters that can reduce mortality rates caused by enveloped viruses is crucial, especially for preventing the spread of infectious diseases. These materials can be used in air and water filtration systems or integrated into sanitation and disinfection technologies, strengthening infection control. They can also serve as highly effective filtration membranes to prevent viral contamination during the production of biopharmaceuticals, ensuring product safety. To find cost-effective materials for filtration and address unsafe drinking water challenges, Mi et al.[6] developed *N*-(2-hydroxy) propyl-3-trimethylammonium chitosan chloride (HTCC)/poly(vinyl alcohol) (PVA) nanofibers. These water-stable fibers demonstrated the ability to efficiently adsorb both enveloped and nonenveloped viruses. In another study, Li et al.[7] created a sialyllactose-functionalized chitosan fiber filter to remove influenza virus from water. The filter's effectiveness was tested using the hemagglutination assay, which showed the filter efficiently removed the virus from the water.

These advancements are especially important for low- to middle-income countries (LMICs), where infectious diseases remain a major challenge. With HIV/AIDS still among the leading causes of death in LMICs[8] and the ongoing effects of

Received: July 30, 2025
Revised: August 8, 2025
Accepted: August 14, 2025

the COVID-19 pandemic, the need for innovative antiviral materials has become more urgent than ever. Biopolymers have emerged as promising options for viral inactivation, offering versatile applications in biopharmaceuticals.[9−13] They possess unique biological properties, including antiviral, antibacterial, antioxidant, anti-inflammatory, and immunomodulatory activities. They are also biodegradable and bioavailable.[14−18] Furthermore, biopolymers can be developed into secondary materials such as nanoparticles (NPs), hydrogels, films, and fibers to meet specific application needs. Nanofibers, in particular, show great promise for filtration purposes compared to traditional filters, due to their higher filtration efficiency, large surface area, small pore sizes, low-pressure drops, and longer lifespan.[19] These qualities make nanofibers ideal for filtering microorganisms since their small pore sizes can trap bacteria and viruses.[20,21] Nanofibers can also be functionalized with antimicrobial agents to boost their effectiveness.[22] There are various methods to produce nanofibers; however, electrospinning is the preferred choice because it is simple and cost-effective.[19,23] It also allows better control over the fiber morphology and orientation. Chitosan was chosen as the primary biopolymer for this study because of its excellent biodegradability and natural antiviral properties, making it a key material in antiviral research.[24,25] A major advantage of chitosan is the reactive amino groups on its glucosamine units, which enable various chemical modifications such as carboxylation, quaternization, sulfation, phosphorylation, thiolation, and acetylation.[26−28] Notably, sulfated chitosan derivatives developed by Artan et al.[25] showed superior antiviral activity compared to unmodified chitosan, highlighting the importance of functionalization in improving therapeutic efficiency.

While numerous studies have examined the antiviral activity of HTCC against enveloped viruses,[29−31] this work introduces a new approach by combining two chitosan derivatives (HTCC and NSC) to create nanoparticles (NPs) that enhance the antiviral effectiveness of these two polymers. Moreover, for the first time, these NPs are integrated into electrospun ethyl cellulose (EC) nanofibers through electrospinning to increase their surface area, thereby developing a potential antiviral filter. This research marks the first investigation into the antiviral activity of NSC, NSC/HTCC NPs, and NSC/HTCC/EC nanofibers against HIV-1. It also opens new avenues for exploring chitosan-based materials in creating advanced antiviral solutions, contributing to existing knowledge. The study aims to develop sophisticated nanofibers capable of neutralizing enveloped viruses. HIV, a retrovirus approximately 100−120 nm in diameter, was used as the model virus to test the filtration system's effectiveness. The anti-HIV activity of the filters was systematically evaluated to determine their capacity to effectively remove or inactivate the virus, ensuring their suitability for long-term biomedical use. Additionally, reusability studies were conducted to assess the stability and potential for reuse of the filters over time. These experiments provided essential insights into the longevity, degradation behavior, and consistent performance of the filters, helping establish optimal reuse conditions and storage protocols for practical applications.

2. EXPERIMENTAL SECTION

2.1. Materials. Chitosan (from shrimp shells, ≥75% deacetylated), glycidyl trimethylammonium chloride (GTMAC), succinic anhydride, ethyl cellulose (EC), dimethyl sulfoxide (DMSO), glacial acetic acid (AcOH), and sodium hydroxide (NaOH) were all purchased from Merck (Pty) (Ltd.), Modderfontein, South Africa. All the other reagents used were of analytical grade. Millipore water was used in all the experiments.

2.2. Synthesis and Characterization of NSC and HTCC. NSC was synthesized following a previously reported procedure with slight modifications.[32] Briefly, chitosan (1.0 g) was dissolved in DMSO (20 mL). Succinic anhydride (0.56 g) was then added to the solution, and the mixture was stirred for 24 h at 60 °C. The pH was adjusted to 12 using NaOH (5% w/v). The product was precipitated in excess acetone and then centrifuged (3000 rpm, 10 min) to remove the acetone. It was washed with ethanol (100 mL, three times) and freeze-dried to obtain the product as a pale yellow powder.

HTCC was also synthesized following a previously reported method.[33] Briefly, 1.0 g of chitosan was dissolved in 250 mL of 0.5% v/v acetic acid solution and stirred for about 3 h until clear. GTMAC was then added in two portions, spaced 1 h apart. After the additions, the mixture was stirred for 24 h at 80 °C. The product was precipitated using excess acetone and centrifuged at 3000 rpm for 30 min to remove the solvent. It was then washed with a 1:1 mixture of acetone and ethanol and freeze-dried to obtain a white foam.

The chemical structures of the synthesized products were analyzed using proton NMR (^{1}H NMR) spectra recorded on a 600 MHz Varian INOVA instrument. The chemical shifts (δ) were reported in parts per million (ppm) downfield, with deuterated water (D_2O) as the solvent.

2.3. Preparation and Characterization. *2.3.1. Preparation of NSC/HTCC NPs and NSC/HTCC/EC Nanofibers.* The NPs were prepared using a previously reported method with slight modifications.[34] HTCC and NSC were dissolved in distilled water to concentrations of 1 and 2 mg/mL, respectively. The solutions were stirred at room temperature until the polymers dissolved completely. HTCC/NSC NPs were prepared by adding 20 mL of the HTCC solution dropwise into 20 mL of the NSC solution. Then, five drops of Tween-80 were added, and the mixture was stirred for 1 h at room temperature. The resulting opalescent solution was dialyzed against deionized water using a dialysis membrane. Finally, the solution was freeze-dried, resulting in a white foam product.

The nanofibers were prepared by dissolving EC in ethanol/deionized water (3:1, v/v) to create an 11 wt % EC solution, which was stirred for 2 h at 80 °C to ensure complete dissolution. The NCS/HTCC NPs were then added to the EC solution to produce solutions with 1, 3, and 5 wt %. Electrospinning was performed using an EC-CLI electrospinning device (IME Technologies, Netherlands), consisting of a high-voltage power supply, a syringe with a needle, a syringe pump, and a cylindrical collector. The distance from the needle tip to the collector was maintained at 15 cm. The voltage was set to 20 kV, and the polymer solution was fed at a flow rate of 3 μL/min. The electrospinning process was conducted at room temperature. The nanofibers were collected on aluminum foil wrapped around the cylindrical collector.

2.3.2. Characterization of NSC/HTCC NPs and Nanofibers. The nanofibers were analyzed using Fourier Transform Infrared Spectroscopy (FTIR) to identify the functional groups in their structure. FTIR analysis was performed with a PerkinElmer Spectrum 100 spectrometer within the 4000 to 600 cm^{-1} range. The average particle size, PDI, and ζ-potential of the HTCC/NSC NPs and nanofibers were measured by dynamic light scattering (DLS) using a Malvern Zetasizer Nano ZS (Malvern Instruments, U.K.). Measurements were taken on diluted samples with deionized water at 25 °C. For the nanofibers, samples were dispersed in deionized water. Each sample was measured three times, and all data are presented as mean ± standard deviation (SD). Transmission electron microscopy (TEM, Zeiss NTS GmbH, Oberkochen, Germany), operated at an acceleration voltage of 200 kV, was used to determine the size of the NSC/HTCC NPs. Samples were prepared by depositing a drop of the NSC/HTCC NPs suspension onto a carbon-coated copper grid and drying at room temperature before observation. The morphology of the nanofibers was examined using the ZEISS EVO scanning electron microscope (SEM), with samples coated in carbon. The

https://doi.org/10.1021/acsanm.5c03567
ACS Appl. Nano Mater. XXXX, XXX, XXX−XXX

Scheme 1. Schematic Reaction of NSC and HTCC with Their Respective ζ-Potential Diagrams

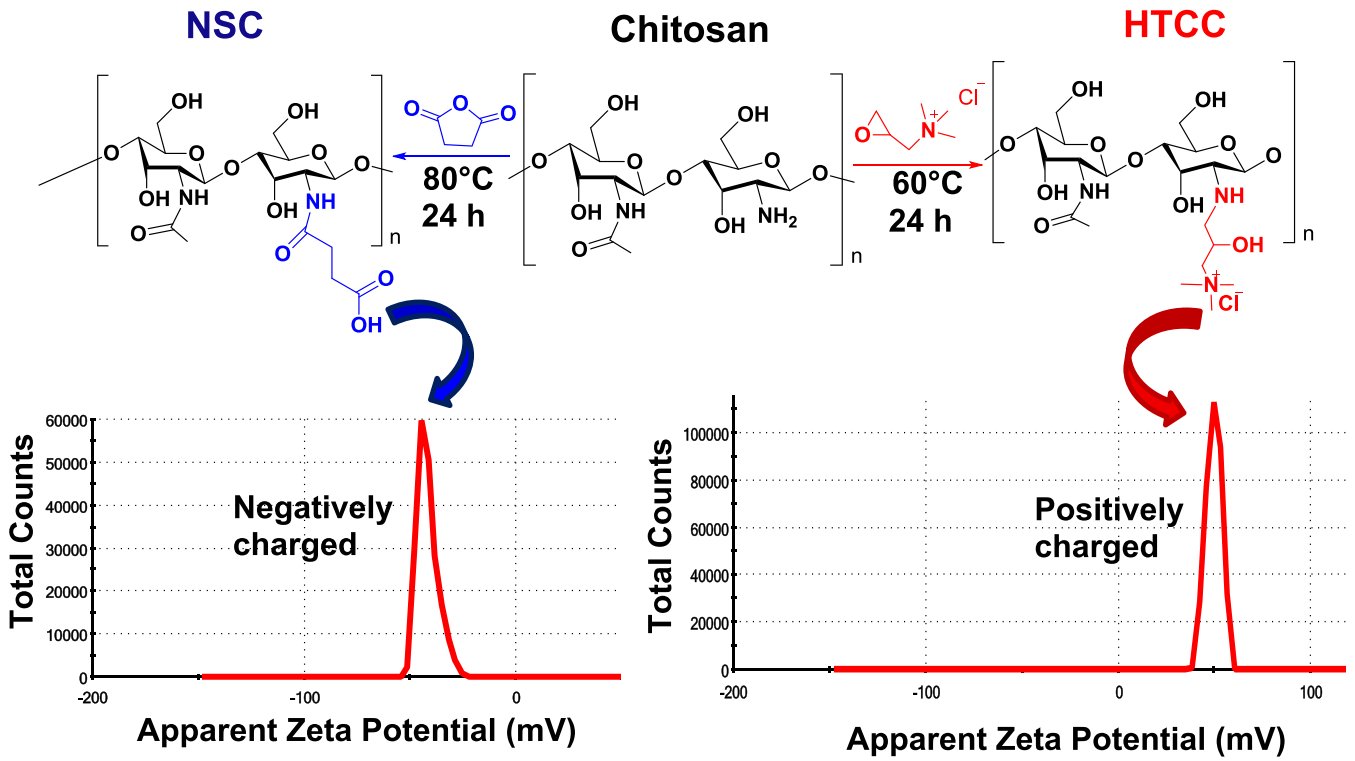

samples were placed in the SEM chamber, and photographic images were captured at an accelerating voltage of 2−5 kV. Fiber diameters were measured by analyzing SEM images with ImageJ software. The Brunauer−Emmett−Teller (BET) surface area and pore size of the nanofibers were determined using a Micromeritics Tristart II (United States) system. Samples were first degassed at 100 °C for 16 h in a nitrogen atmosphere, then analyzed using N_2 adsorption at 77° K.

2.4. Antiviral Activity against Pseudo-HIV Virus. *2.4.1. Cytotoxicity Assay.* The cytotoxicity assay for the compounds was performed using a previous method.[31] The assay for the columns started by seeding 10,000 cells per well in 100 μL of TZM-bl cells in a 96-well plate, which was incubated for 24 h at 37 °C and 5% CO_2. After incubation, 100 μL of media was applied to each column for 30 min, then the solution was added to the cells, except in the control wells. After 48 h, the media was removed and replaced with 25 μL of 3-(4,5-dimethylthiazol-2-yl)-2,5-diphenyltetrazolium bromide (MTT) reagent at 5 mg/mL (Thermo Fisher Scientific, United States). The cells were incubated at 37 °C for 3 h to allow formazan to form from viable cells. Then, the MTT was removed, and 100 μL of DMSO was added to the cells and incubated for 15 min at room temperature. After this, the plates were read at 620 nm using the Tecan Infinite luminometer (Tecan, Switzerland).

2.4.2. Generation of HIV-1 Subtype C Pseudovirus. The HIV-1 CAP210.2.00.E8 subtype C pseudovirus was produced using a previous method.[31] It was generated by cotransfecting an envelope-containing plasmid (PSG-3Δenv) with a plasmid carrying the luciferase reporter gene[35] into 2 × 10^6 HEK 293T cells in 10 mL of growth media using the X-tremeGENE transfection reagent (Sigma-Aldrich, United States). The virus stock's $TCID_{50}$ was determined by infecting TZM-bl cells with serial 4-fold dilutions of the supernatant in quadruplicate in the presence of DEAE dextran (37.5 μg/mL) (Sigma-Aldrich, St. Louis, MO). After 48 h, the Bright Glo Reagent (Promega, Madison, WI) was used to assess infection, and luminescence was measured with a Tecan Infinite.

2.4.3. The Inhibition of HIV-1 Subtype C Infection of TZM-bl Cells. The method previously used was followed.[31] Briefly, experiments were conducted in duplicate using 96-well flat-bottom plates. Dulbecco's Modified Eagle Medium (DMEM) with fetal bovine serum (FBS) (Thermo Fisher Scientific, United States) growth media (100 μL) was added to each well, with 150 μL added to the control wells. A 3-fold serial dilution of the samples was performed, and then 50 μL of CAP210.2.00.E8 pseudovirus was added to the wells. The plates were incubated for 1 h at 37 °C to allow interaction between the samples and the pseudovirus. TZM-bl cells (10,000 cells/well in 100 μL) were then added and incubated for 48 h at 37 °C with 5% CO2. After incubation, 150 μL of media was removed from each well, and Bright-Glo Luciferase substrate (Promega; United States) was added, followed by a 2 min incubation. Subsequently, 150 μL was transferred to black 96-well plates, and luminescence was measured using the Tecan Infinity F500. Infection levels were recorded as Relative Light Units (RLU).

2.4.4. Preparation of HIV-1 Filter and the Anti-HIV Studies for the filters. The anti-HIV assay for the filters was performed as described in Section 2.4.3, with minor modifications.

The filter was prepared using a 1 mL syringe; the prepared fibers were stacked inside the syringe until reaching 0.1 mL (Figure S1, Supporting Information). The pseudovirus was then added to the syringe and allowed to flow through for 30 min. Next, 50 μL of the contents was transferred to a 96-well plate containing 10,000 TZM-bl cells/200 μL/well. The experiment was incubated for 48 h at 37 °C with 5% CO_2. After incubation, 150 μL of media was removed from the plate, and 100 μL of Bright-Glo Luciferase was added and incubated for 2 min. Then, 150 μL was transferred to a corresponding black plate, and luminescence was measured using a TECAN 500 plate reader.

2.4.5. Anti-HIV Time Studies Using Subtype C Pseudovirus. The time studies were conducted to determine how long it takes for the samples and filters to demonstrate effectiveness against the virus. This study involved incubating the sample with the virus at various time intervals before infecting the target TZM-bl cells, as outlined in the HIV neutralization assay above. The tested time intervals included 20, 40 s, 1, 2, 3, 4, and 5 min of virus and sample incubation. After infecting the target TZM-bl cells, the incubations were performed as described above. The relative light unit was also measured as previously mentioned.

2.4.6. The Reusability and Performance Stability of the Anti-HIV Filter Material. The filters' material was tested for reusability, meaning how many times the filter can be used while remaining

https://doi.org/10.1021/acsanm.5c03567
ACS Appl. Nano Mater. XXXX, XXX, XXX−XXX

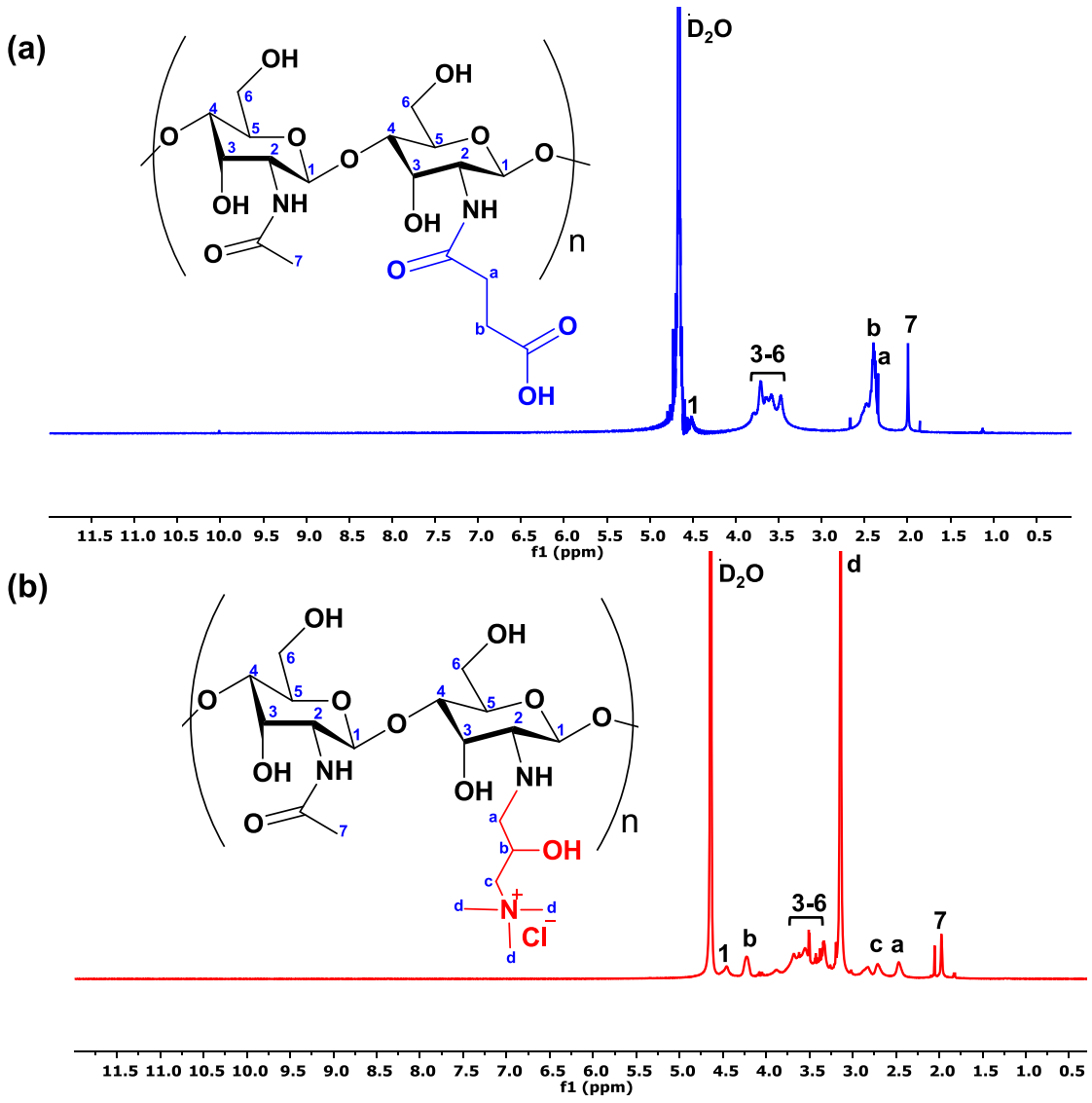

Figure 1. ^{1}H NMR spectrum of (a) NSC and (b) HTCC in D_2O performed at 30 °C.

effective against HIV. The study aimed to test the material repeatedly until no HIV inhibition was detected. The filter was loaded with the virus in the material for 3−5 min before infecting the cells. After incubation with the virus, the columns were allowed to dry for 2 days in the fume hood. The experimental incubations and RLU measurements were performed as described above.

3. RESULTS AND DISCUSSION

3.1. Synthesis and Characterization of NSC and HTCC. Chitosan can easily be modified into a wide range of chemical derivatives due to the reactive amino groups on the glucosamine units. This property makes it highly attractive, as it can be tailored to have specific properties for various applications. This study modified chitosan to enhance its solubility and antiviral activity by conjugating it with succinic anhydride and GTMAC to form NSC and HTCC, respectively. NSC was produced through a ring-opening reaction by attaching succinyl groups to the primary amino groups of glucosamine units, forming amide bonds as shown in Scheme 1. NSC carried an overall negative charge because of the carboxylate ions (COO−) created by the ionization of the carboxyl (COOH) groups in solution.[36] In contrast, HTCC had a quaternary ammonium group introduced onto the chitosan backbone via an alkylation reaction, as shown in Scheme 1. This modification gave HTCC a permanent positive charge, independent of the pH of the water.[37] The ζ-potential of NSC and HTCC was measured to be −42 ± 3.32 and 49 ± 2.21, respectively (Scheme 1).

The ^{1}H NMR spectra were used to confirm the chemical structures of NSC and HTCC, as shown in Figure 1. The chemical shifts at 2.0 ppm (H_7), 3.18 ppm (H_2), 3.6−3.89 ppm (H_3, H_4, H_5, and H_6), and 4.5 ppm (H_1) were attributed to chitosan protons (Figure S2, Supporting Information). Two new peaks appeared in the ^{1}H NMR spectra of NSC, corresponding to the succinyl group. The peaks at 2.45 and 2.47 ppm were assigned to H_a (−NH(CO)−CH_2−) and H_b (−CH2−COOH), respectively. Similarly, in the ^{1}H NMR spectra of HTCC, two new peaks indicated successful grafting of GTMAC onto the chitosan backbone. The chemical shift at 3.2 ppm was assigned to trimethylammonium protons (H_d), and the shift at 2.8 ppm was assigned to methylene group protons (H_c). These results align with existing literature.[38−43]

3.2. Synthesis and Characterization of NSC/HTCC NPs. The NSC/HTCC nanoparticles were synthesized using

https://doi.org/10.1021/acsanm.5c03567
ACS Appl. Nano Mater. XXXX, XXX, XXX−XXX

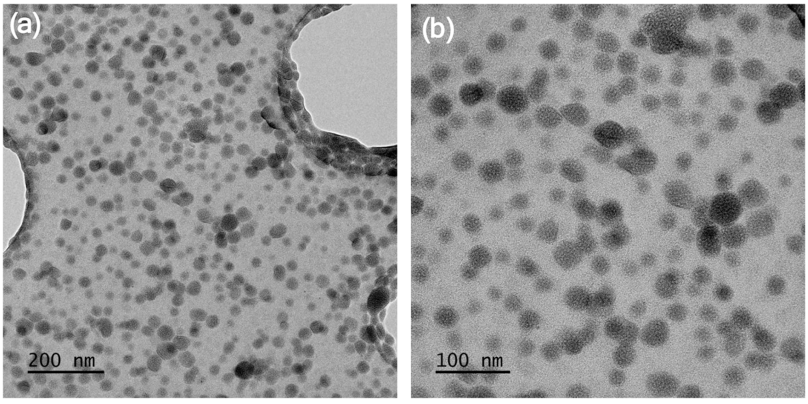

Figure 2. TEM micrographs at (a) 200 nm and (b) 100 nm of NSC/HTCC NPs.

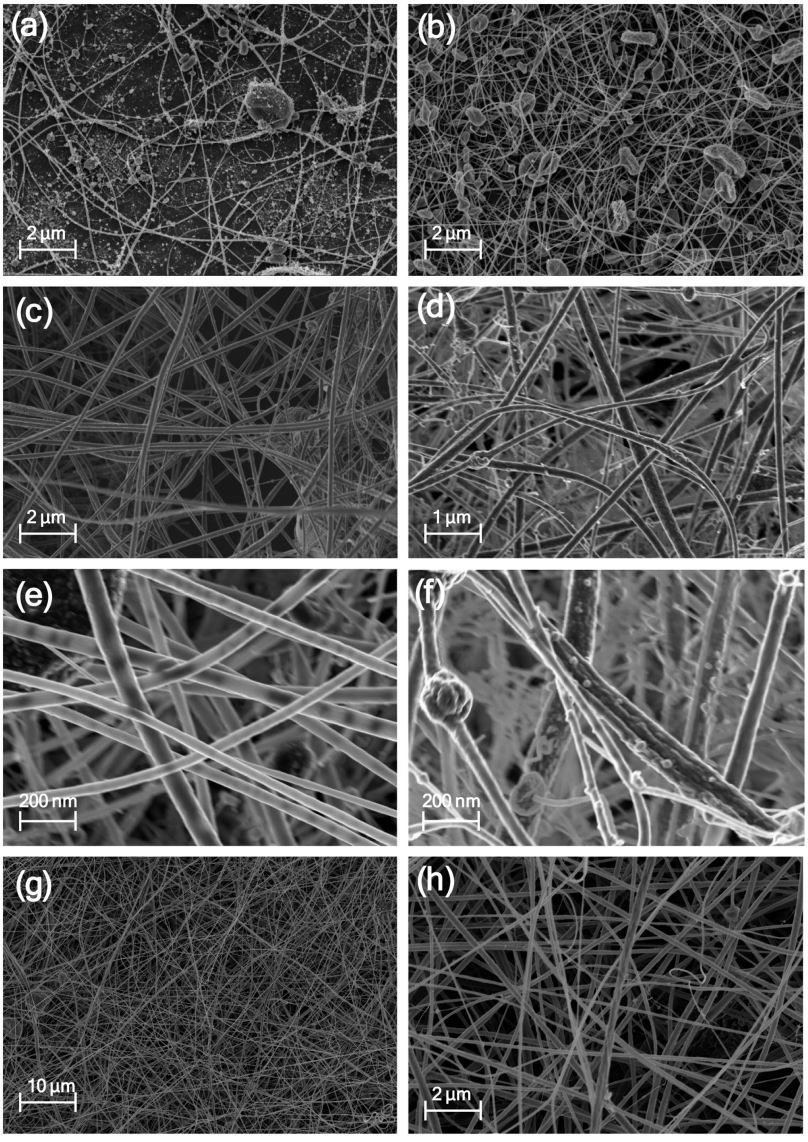

Figure 3. SEM micrographs of (a) 6 wt % EC nanofibers at 15 kV, (b) 11 wt % EC nanofibers at 15 kV, (c) 11 wt % EC nanofibers at 20 kV, (d) 5% NSC/HTCC/EC nanofibers at 3 μL/min and 20 kV, (e) 5% NSC/HTCC/EC nanofibers at 20 kV showing 200 nm NPs inside the fibers, (f) 5% NSC/HTCC/EC nanofibers at 20 kV with 200 nm NPs on the surface of the fibers, (g) 5% NSC/HTCC/EC nanofibers at 2 μL/min and 20 kV with a scale of 10 μm, and (h) 5% NSC/HTCC/EC nanofibers at 2 μL/min and 20 kV with a scale of 2 μm.

polyelectrolyte complexation, an effective method that eliminates the need for cross-linking agents.[44] In this process, cross-linking occurs through ionic interactions between the negatively charged NSC and positively charged HTCC,

https://doi.org/10.1021/acsanm.5c03567
ACS Appl. Nano Mater. XXXX, XXX, XXX−XXX

forming stable nanoparticles. When the two solutions were mixed, an opalescent appearance was observed, indicating successful nanoparticle formation. Various ratios of NSC to HTCC at different concentrations were tested, maintaining ratios between 1:1 and 1:1.5, as higher ratios resulted in larger particle sizes. The solutions were also added dropwise to prevent the formation of larger particles. Literature shows that HIV viral particles can be relatively small. For example, Bricks et al.[45] reported an average size of 145 nm for an HIV-1 virion in their study. Therefore, the targeted size for this study was less than 100 nm. The final size, PDI, and ζ-potential were measured as 41 ± 2.1 nm, 0.21 ± 0.029, and −24 ± 1.20 mV, respectively (Figure S3, Supporting Information).

TEM was also used to determine the average size and shape of the NPs, which showed a spherical form with no signs of agglomeration, as shown in Figure 2. The particle size distribution histogram from TEM indicated that the NPs ranged from 15 to 50 nm in size, with an average diameter of 33 nm (Figure S4, Supporting Information). These findings matched the results obtained with DLS; however, the DLS data were slightly higher compared to TEM results. The difference between the two methods is expected, as the measurement principles differ. DLS measures the hydrodynamic size of the nanoparticle, including the surrounding solvent layer, while TEM measures the actual size of the nanoparticle in a dry state. Therefore, TEM measurements may result in smaller particle sizes than DLS measurements.[46]

3.3. Synthesis and Characterization of NSC/HTCC/EC Nanofibers. *3.3.1. Morphology and Size of the Nanofibers.* EC was used as the matrix to fabricate nanofibers because of its nontoxic, biocompatible, biodegradable, and low water-solubility properties.[47,48] To examine the effect of solution concentration on nanofiber formation, solutions of 6 and 11 wt % were prepared in ethanol/water (3:1), and nanofibers were electrospun at a voltage of 15 kV, a flow rate of 4 μL/min, and a distance of 10 cm. As shown in Figure 3(a), only small fibers with many clusters formed at 6 wt %, indicating insufficient polymer chain entanglement due to low solution viscosity, which hampers the polymer chains' ability to resist stretching during electrospinning.[49] These findings align with those of Borrego et al.[47] who demonstrated that EC fibers formed below 8 wt % contain defects, particles, and clusters, while fibers formed above 8 wt % were defect-free. Increasing the concentration to 11 wt % ultimately produced uniform fibers averaging 230 nm in diameter (Figure S5, Supporting Information); however, these fibers still contained beads, as shown in Figure 3(b). Bead formation likely resulted from a smaller distance combined with a high flow rate, which causes some fibers not to dry completely before reaching the collector. Uniform, bead-free fibers were finally obtained at a flow rate of 3 μL/min, with a voltage of 20 kV, at a distance of 15 cm, as depicted in Figure 3(c). Similar results were reported by Nugraha et al.[50] who fabricated PVDF (Polyvinylidene Fluoride) nanofibers; at 10−16 kV, beads formed on the fibers, while increasing the voltage to 20 kV resulted in smooth, uniform fibers without beads. NSC/HTCC NPs were added to the EC nanofibers; Figure 3(d) shows 5% NSC/HTCC/EC nanofibers, which were not uniform and contained some beads. Figure 3(e),(f) show the nanofibers at 200 nm magnification for better clarity: some NPs were embedded within the fiber's continuous network (Figure 3(e)), while others aggregated on the surface (Figure 3(f)). In their study, Zienkiewicz-Strzałka et al.[51] fabricated chitosan nanofibers with a silica phase and incorporated silver NPs; these NPs were randomly distributed on the fiber surface, similar to the results in this study. The 5% NSC/HTCC/EC nanofibers were further optimized by reducing the flow rate to 2 μL/min while maintaining other parameters, resulting in uniform fibers without beads with an average diameter of 210 nm, as shown in Figure S6 (Supporting Information), and visualized at 10 μm (Figure 3(g)) and 2 μm (Figure 3(h)).

3.3.2. FTIR Analysis of the Nanofiber Membranes. FTIR spectroscopy confirmed the incorporation of NSC/HTCC NPs into EC nanofibers by analyzing the intensity and wavenumber shift of the vibrations. The FTIR spectra of chitosan, HTCC, NSC, and NSC/HTCC NPs are shown in Figure S7 (Supporting Information). As shown in Figure 4,

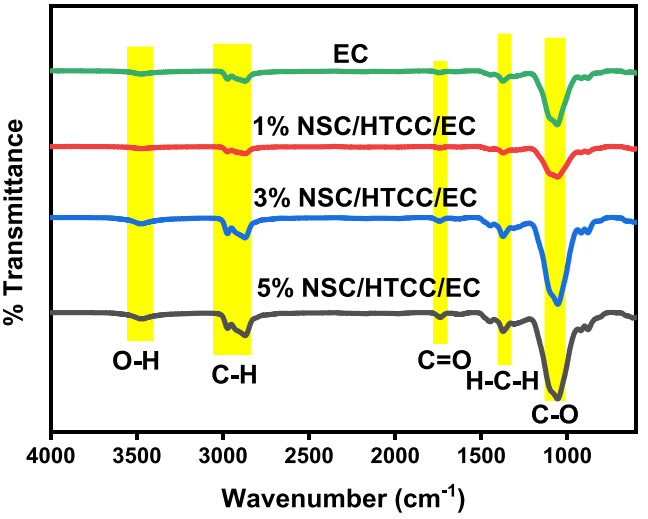

Figure 4. FTIR spectra of EC, 1% NSC/HTCC/EC, 3% NSC/HTCC/EC, and 5% NSC/HTCC/EC nanofibers.

adding 1% of the NPs did not cause significant changes in peak intensity or wavenumber shift. However, notable changes were observed with 3 and 5% NP incorporation; the OH stretching vibration at 3477 cm^{-1} broadened as the NP amount increased. This occurs because the NPs already contain hydroxyl groups; thus, adding NPs increases the OH content in the nanofibers. Similar patterns appeared in the stretching vibrations at 2868−2983, 1050, and 1370 cm^{-1}, linked to CH, glycosidic bonds, and CH_2 stretching vibrations, respectively. Likewise, Wu et al.[52] created PVA/HTCC nanofibers, and adding chitosan and HTCC to PVA increased peak intensity, especially the OH peak. In another study, Nordi et al.[53] synthesized TPU nanocomposites reinforced with jute cellulose nanofibers (CNFs). Their FTIR analysis showed that certain stretching vibration bands increased when they incorporated 2 and 4% jute CNFs into the TPU. The rise in peak intensity in these functional groups was due to the addition of NPs, which also have similar functional groups. The weak vibration at 1730 cm^{-1} became more prominent as concentration increased, attributed to the C═O carbonyl group in the NPs, stemming from the carboxylic groups in NSC. In their study, Alekseeva et al.[54] confirmed the small band at 1735 cm^{-1}, indicating the presence of C═O in small quantities in the polymer. These findings suggest the successful incorporation of NPs into the EC nanofibers. The absence of wavenumber shifts indicates no chemical interaction between EC and the NPs. However, the increased peak intensity

https://doi.org/10.1021/acsanm.5c03567
ACS Appl. Nano Mater. XXXX, XXX, XXX−XXX

demonstrates that NPs have been successfully integrated into the nanofibers.

3.3.3. Surface Charge of the Nanofibers. The surface charge of the nanofibers was also measured using DLS, as it significantly influences their performance in filtration applications. Nanofibers with specific surface charges have been shown to capture charged particles and improve filtration efficiency. For example, a filter material with a negative surface charge will strongly interact electrostatically with positively charged pathogens.[21,55] This helps prevent the pathogens from passing through the filter. The surface charge of EC, 1% NSC/HTCC/EC, 3% NSC/HTCC/EC, and 5% NSC/HTCC/EC nanofibers was measured to be −23 ± 0.946, −33 ± 3.58, −42 ± 2.41, and −48 ± 1.63 mV, respectively. As expected, increasing the concentration of NPs raised the surface charge because the NPs have a negative surface charge. Similar findings were reported by Ghiasi et al.[56] In their study, they created ultrafiltration membranes using a poly(ether sulfone)/polyimide blend. Polyimide is a negatively charged polymer, so increasing the polyimide content made the membranes more negatively charged. The formulation with the highest polyimide content (with a surface charge of −61.5 mV) showed the best performance, rejecting 99.9% of bovine serum albumin (BSA).[56]

3.3.4. Surface Area Analysis. The surface area of the NPs was increased by embedding them within the nanofiber matrix, making them more exposed. The surface area, pore size, and pore volume of the nanofibers were measured using BET analysis, as these are key factors in filtration applications. These properties influence the selectivity, efficiency, and adsorption capacity of the filters. The BET results are summarized in Table 1. The surface area of the nanofibers ranged from 13.24 to 16.635 m^2/g. These findings are similar to a study by Hao et al.[57] who reported a surface area ranging from 5.91 to 16.90 m^2/g for EC fibers. Similarly, Chen et al.[58] in their study with wheat straw cellulose nanofibers, found a surface area of 16.5 m^2/g and a pore size of 6.3 nm. Higher surface areas are essential for filter efficiency because they provide more space for virus adsorption and reduce clogging. The pore sizes ranged from 4.48 to 7.01 nm, which falls within the 1−10 nm range typically expected for ultrafiltration membranes.[59] Smaller pores are preferable because they can trap smaller particles, increasing the filter's efficiency. The increase in pore size with higher concentrations of NSC/HTCC NPs, as shown in Table 1, is due to the increased viscosity of the polymer solution. As more NPs are added to the EC solution, the viscosity rises, resulting in fibers with larger diameters and, consequently, larger pores. Similar results were observed by Chen et al.[60] who studied the effect of solution viscosity and composition on electrospinning nanoporous PCL microtubes. They found that higher viscosity in the core and sheath solutions led to larger microtube diameters and larger pore sizes.

Table 1. BET Analysis Results of the Electrospun Fibrous Membranes

nanofiber	BET surface area (m^2/g)	pore size (nm)
NSC/HTCC NPs	7.817	1.732
EC	16.63	4.494
5% NSC/HTCC/EC	16.05	7.012
3% NSC/HTCC/EC	13.69	6.201
1% NSC/HTCC/EC	13.24	4.487

3.4. Antiviral Activity against HIV-1 Subtype C.

3.4.1. The Antiviral Activity of NSC, HTCC, and NSC/HTCC NPs. The cytotoxicity of the polymers was assessed on TZM-bl cells using MTT proliferation assays (Figure S8, Supporting Information) to confirm that all inhibition tests were conducted at nontoxic levels. The cytotoxicity percentages for chitosan, HTCC, and NSC/HTCC NPs were 31, 23, and 34%, respectively. NSC showed no toxicity. As shown in Table 2, since the cytotoxicity of all tested polymers stayed below 50%, the CC_{50} (concentration killing 50% of cells) could not be determined. Therefore, the CC_{50} value is greater than the highest tested concentration of 0.333 mg/mL. Based on these results, all tested polymers are considered nontoxic to the target cells.

Table 2. Cytotoxicity and Inhibitory Concentrations in mg/mL of the Polymers at 50% against HIV-1 Subtype C on TZM-bl Cells

		subtype C
polymer	cell cytotoxicity at 50% (CC_{50})	Inhibition concentration at 50% (IC_{50})
NSC	-	0.156
HTCC	-	0.279
NSC/HTCC	-	0.0023

The luciferase-based antiviral assay was performed to evaluate the antiviral activity of the polymers against HIV-1 subtype C pseudovirus, as subtype C is the most prevalent compared to subtypes A and B. As shown in Figure 5(a), chitosan did not demonstrate any inhibition of HIV-1; this may be because the concentrations used in the inhibition studies are low, with the highest tested concentration being 0.333 mg/mL. Wu et al.[61] also examined the antiviral activity of chitosan against HIV-1. Chitosan did not exhibit any inhibition at concentrations of 0.1 and 0.25 mg/mL. Another study by Cele et al.[62] reported 53% inhibition activity for chitosan against HIV-1 at a concentration of 120 mg/mL, which is relatively high compared to the concentrations tested here. In a different study by Artan et al.[25] using chitooligosaccharides, no activity against HIV-1 was observed, even at the highest tested concentration. However, modified chitosan derivatives showed improved antiviral activity compared to chitosan. NSC demonstrated strong inhibition activity compared to HTCC, with 82% inhibition against subtype C at the highest tested concentration. The way NSC inhibits HIV-1 is believed to be similar to sulfated chitosan derivatives, as it is negatively charged. According to Sosa et al.[63] N-carboxymethylchitosan−N-O-sulfate, a chitosan sulfate derivative, inhibits HIV-1 by blocking the interaction between HIV-1 gp120 and CD^{4+} cell surface receptors and by reverse transcribing the viral genome. Therefore, NSC's activity can likely be attributed to electrostatic interactions between the negative carboxylate ions in NSC and the positively charged amino acids in HIV-1 gp120, leading to shielding and preventing the virus from binding to the cell surface.[24] HTCC did not exhibit strong inhibition, with only 54% inhibition against subtype C at the highest tested concentration.

NSC and HTCC were combined by nanosizing them to evaluate their synergistic antiviral activity against HIV-1. This

https://doi.org/10.1021/acsanm.5c03567
ACS Appl. Nano Mater. XXXX, XXX, XXX−XXX

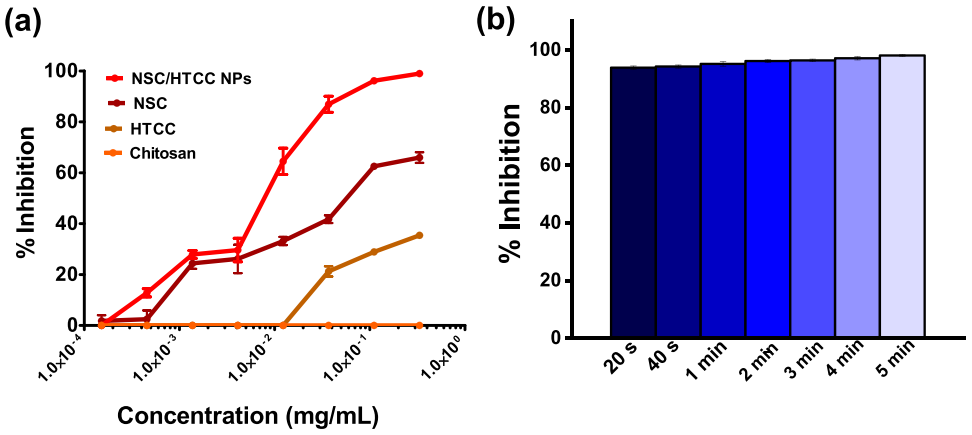

Figure 5. Evaluation of the anti-HIV activity of chitosan, modified chitosan, and the NPs against HIV-1 subtype C pseudovirus: (a) Neutralization inhibition assays and (b) neutralization inhibition assays at different time points. The error bars indicate the mean ± standard deviation.

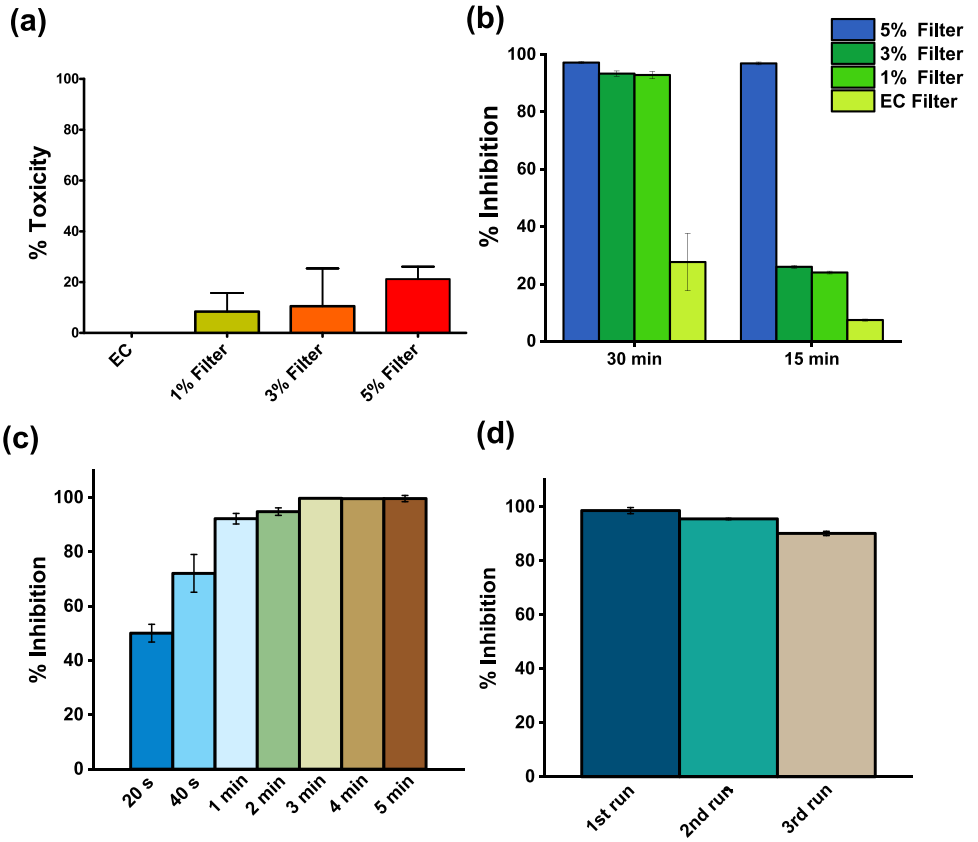

Figure 6. (a) The cytotoxicity activity of the anti-HIV filters against TZM-bl cells. (b) The anti-HIV activity of the filters against HIV-1 subtype C. (c) Time studies of the 5% NSC/HTCC/EC filter against HIV-1 subtype C pseudovirus. (d) Reusability evaluation of the 5% NSC/HTCC/EC filter against HIV-1 subtype C pseudovirus. The error bars represent the mean ± standard deviation.

combination significantly enhanced inhibition, reaching nearly 100% against the pseudo-HIV subtype C virus. The high antiviral effectiveness of the NSC/HTCC NPs can be attributed to the inherent antiviral properties of both components, although HTCC alone shows relatively lower activity. The improved anti-HIV activity is linked to the fact that the materials are nanosized. Nanosized materials tend to have a larger surface area compared to their bulk counterparts, allowing for more interactions with HIV-1 viral particles. Additionally, due to their small size, NPs can penetrate cells more easily and interact with intracellular viruses, making them effective in targeting viruses within host cells, which traditional materials might not reach. Similar results were obtained in our previous study, where HTCC did not show strong anti-HIV activity; however, after nanosizing, its antiviral activity increased significantly.[31] The NSC/HTCC also showed good antiviral activity against SARS-CoV-2 (Figure S9, Supporting Information).

Since the intended application of this study is to develop an antiviral filter against enveloped viruses, time studies were conducted to ensure that using these NPs would be practical, as a material that can inhibit the virus quickly would be beneficial for the intended purpose. The HIV-1 subtype C virus was incubated with the NCS/HTCC NPs at different

https://doi.org/10.1021/acsanm.5c03567
ACS Appl. Nano Mater. XXXX, XXX, XXX−XXX

intervals to determine how rapidly the NPs inhibit the virus. As shown in Figure 5(b), the NPs achieved 95% inhibition within 20 s of incubation. The results were promising, indicating that the NPs would be suitable for the intended application if they demonstrate strong anti-HIV activity within 20 s.

3.4.2. The Antiviral Activity of the Antiviral Filters. The cytotoxicity profile of the antiviral filters was also tested using TZM-bl target cells. EC and 1% NSC/HTCC/EC filters showed no toxicity to the target cells, as illustrated in Figure 6(a). However, the 3 and 5% NSC/HTCC/EC filters exhibited toxicity levels of 5 and 20%, respectively. Overall, the anti-HIV filters did not display significant toxicity toward the target cells. Microscopic images of the cells before and after treatment with the filters were captured. The similarity in cell appearance before and after treatment confirms that the filters are nontoxic to the cells (Figure S10, Supporting Information). These findings align with previous results, as it has been shown that EC is not toxic. In fact, EC has been widely recognized as safe (GRAS) and approved by the FDA for use in pharmaceuticals and as a food additive.[64] Krasian et al.[65] studied the cytotoxicity of EC membranes and found that EC membranes were not toxic to the tested cell line, even after 72 h, indicating a low risk of prolonged effects. Another benefit of using EC is its biodegradability compared to other common filter materials, such as ceramics or synthetic filters.[66]

The anti-HIV activity of the filters was tested against HIV-1 CAP210.2.00.E8 subtype C pseudovirus. The virus was incubated with the filters for 30 and 15 min, as shown in Figure 6(b). The filters showed nearly 100% inhibition at 30 min, except for the EC filter, which did not demonstrate significant inhibition against the pseudovirus. However, no significant inhibition was seen at 15 min for EC, 1 and 3% NSC/HTCC/EC filters. The lack of activity in these filters is likely due to the short incubation time; more prolonged incubation generally enhances activity. Results indicate that the antiviral effect is related to the addition of NSC/HTCC, with the highest activity observed in the filter containing the highest concentration of nanoparticles (NPs). The 5% NSC/HTCC/EC membrane also had the highest surface charge, as described in Section 3.3.3. Therefore, the filters inhibit subtype C pseudovirus through virus binding to the NPs. Similar findings were reported by Li et al.[7] who developed a filter by packing fibers into the bottom of a sterilized 1 mL syringe. When the HIV suspended in PBS was passed through this filter, it captured nearly 100% of the virus. In another study, Akin et al.[67] created bioselective PVDF membranes via chitosan surface modification to capture hepatitis A virus, removing 99.99% of the virus from water samples. Due to its potent antiviral activity, only the 5% NSC/HTCC/EC filter was used in further experiments.

To assess how quickly the filter (5% NSC/HTCC/EC) inhibited the subtype C virus, the virus was incubated in the filter at various time points. The results showed that the filter achieved 50% inhibition after 20 s and over 70% after 40 s. From 1 to 5 min, the filter demonstrated over 80% inhibition of the virus (Figure 6(c)). Therefore, the 5% NSC/HTCC/EC filter was effective against HIV-1 subtype C within 40 s of contact. Its ability to inhibit the virus rapidly makes it an attractive antiviral filter for enveloped viruses. Given the remarkable activity of the 5% NSC/HTCC/EC filter against HIV-1 subtype C within seconds, the next step was to evaluate its reusability and performance stability—specifically, how many times it could be reused before losing efficacy. Results indicated that the first use achieved 99% inhibition, the second 96%, and the third 90% (Figure 6(d)). This trend suggests a gradual decline in antiviral activity with repeated use, especially after 2 days of drying between cycles. The study was limited to three cycles, as further use caused filter degradation and contamination. To extend the filter's lifespan, increasing the antibacterial agent concentration could help maintain sterility and effectiveness. Future studies might focus on increasing the concentration of HTCC during nanoparticle synthesis, as it has demonstrated strong antibacterial properties. Wu et al.[68] fabricated PVA/HTCC nanofibers cross-linked with blocked diisocyanate, which showed excellent antibacterial activity against *Escherichia coli* with 100% efficacy. Similarly, Cheah et al.[69] developed P-HTCC membranes via electrospinning, which achieved up to 99.95% antibacterial activity against *E. coli*, indicating its potential for microfiltration applications to efficiently disinfect *E. coli*. Based on these findings, the 5% NSC/HTCC/EC filter shows significant promise as an affordable, reusable HIV-1 filtration system.

4. CONCLUSIONS

This study reported the successful fabrication of NSC/HTCC/EC nanofibers through electrospinning to evaluate their synergistic effect as a potential antiviral filter against enveloped viruses. These filters showed promising results. The antiviral filters effectively inhibited HIV-1 infection within a few seconds, while showing no toxicity against the tested cell line. Moreover, the filters maintained good antiviral activity even after being used three times. These findings are encouraging, especially considering that only a 5% concentration of the nanoparticles was used. Future studies will focus on enhancing the reusability of the filters. These filters can be further optimized for future applications, such as HIV-1 filters for breast milk and blood filtration. This study provides a strong foundation for future research on enveloped viruses, with potential applications of the developed nanofibers in various antiviral strategies. These promising materials could be used in real-world applications as cost-effective measures for controlling enveloped viruses.

■ ASSOCIATED CONTENT

Supporting Information

The Supporting Information is available free of charge at https://pubs.acs.org/doi/10.1021/acsanm.5c03567.

The prepared NSC/HTCC/EC filter, chitosan ^{1}H NMR, NSC/HTCC NPs particle size and ζ-potential distribution, NSC/HTCC NPs particle size distribution histogram, EC size distribution histogram, 5% NSC/HTCC/EC nanofiber size distribution histogram, FTIR spectra of chitosan, HTCC, NSC, and NSC/HTCC NPs, cytotoxicity evaluation of chitosan, NSC, HTCC, and NSC/HTCC NPs, neutralization assays of NSC/HTCC NPs against SARs-CoV-2, and microscopic images of TZM-bl cells before and after treatment with the filters (PDF)

■ AUTHOR INFORMATION

Corresponding Authors

Lesego Tshweu − *Centre for Nanostructures and Advanced Materials, DSI-CSIR Nanotechnology Innovation Centre, Council for Scientific and Industrial Research, Pretoria 0001, South Africa; Material Science, Innovation and Modelling*

https://doi.org/10.1021/acsanm.5c03567
ACS Appl. Nano Mater. XXXX, XXX, XXX−XXX

(MaSIM), Faculty of Natural and Agricultural Sciences, North-West University, Mmabatho 2735, South Africa; Email: ltshweu@csir.co.za

Suprakas Sinha Ray − *Centre for Nanostructures and Advanced Materials, DSI-CSIR Nanotechnology Innovation Centre, Council for Scientific and Industrial Research, Pretoria 0001, South Africa; Department of Chemical Sciences, University of Johannesburg, 2028 Johannesburg, South Africa*; orcid.org/0000-0002-0007-2595; Email: rsuprakas@csir.co.za

Authors

Khanyisile S. Dhlamini − *Centre for Nanostructures and Advanced Materials, DSI-CSIR Nanotechnology Innovation Centre, Council for Scientific and Industrial Research, Pretoria 0001, South Africa; Department of Chemical Sciences, University of Johannesburg, 2028 Johannesburg, South Africa*

Cyril T. Selepe − *Centre for Nanostructures and Advanced Materials, DSI-CSIR Nanotechnology Innovation Centre, Council for Scientific and Industrial Research, Pretoria 0001, South Africa; Department of Chemical Sciences, University of Johannesburg, 2028 Johannesburg, South Africa*

Bathabile Ramalapa − *Centre for Nanostructures and Advanced Materials, DSI-CSIR Nanotechnology Innovation Centre, Council for Scientific and Industrial Research, Pretoria 0001, South Africa; Material Science, Innovation and Modelling (MaSIM), Faculty of Natural and Agricultural Sciences, North-West University, Mmabatho 2735, South Africa*

Krishna K. Govender − *Department of Chemical Sciences, University of Johannesburg, 2028 Johannesburg, South Africa*; orcid.org/0000-0002-9058-1675

Complete contact information is available at: https://pubs.acs.org/10.1021/acsanm.5c03567

Author Contributions

K.S.D.: Conceptualization, formal analysis, validation, data curation, writing—original draft, writing—review, and editing. C.T.S.: Biological tests, methodology, data curation, formal analysis, writing—review, and editing. B.R.: Biological tests, methodology, data curation, formal analysis, writing—review, and editing. K.K.G.: Conceptualization, investigation, methodology, formal analysis, validation, data curation, supervision, writing—original draft, writing—review, and editing. L.T.: Conceptualization, investigation, methodology, formal analysis, validation, data curation, supervision, writing—original draft, writing—review, and editing. S.S.R.: Conceptualization, investigation, methodology, formal analysis, validation, data curation, supervision, writing—original draft, writing—review, editing, and funding acquisition. All authors have read and agreed to the published version of the manuscript.

Notes

The authors declare no competing financial interest.

■ ACKNOWLEDGMENTS

The authors would like to acknowledge the financial support from the Department of Science and Innovation (C6A0058), the Council for Scientific and Industrial Research in Pretoria (086ADMIN), and the University of Johannesburg (086310), South Africa.

■ REFERENCES

(1) Zeng, L.; Li, J.; Lv, M.; Li, Z.; Yao, L.; Gao, J.; Wu, Q.; Wang, Z.; Yang, X.; Tang, G.; Qu, G.; Jiang, G. Environmental Stability and Transmissibility of Enveloped Viruses at Varied Animate and Inanimate Interfaces. *Environ. Health* **2023**, *1*, 15−31.

(2) Chaqroun, A.; Bertrand, I.; Wurtzer, S.; Moulin, L.; Boni, M.; Soubies, S.; Boudaud, N.; Gantzer, C. Assessing Infectivity of Emerging Enveloped Viruses in Wastewater and Sewage Sludge: Relevance and Procedures. *Sci. Total Environ.* **2024**, *943*, No. 173648.

(3) Martini, M.; Gazzaniga, V.; Bragazzi, N. L.; Barberis, I. The Spanish Influenza Pandemic: A Lesson from History 100 Years after 1918. *J. Prev. Med. Hyg.* **2019**, *60*, E64−E67.

(4) del Rio, C. The Global HIV Epidemic: What the Pathologist Needs to Know. *Semin. Diagn. Pathol.* **2017**, *34*, 314−317.

(5) World Health Organization. COVID-19 Weekly Epidemiological Update March 2023. https://www.who.int/publications/m/item/weekly-epidemiological-update-on-covid-19---1-march-2023. (Date accessed: February 15, 2025).

(6) Mi, X.; Vijayaragavan, K. S.; Heldt, C. L. Virus adsorption of water stable querternized xhitosan nanofibers. *Carbohydr. Res.* **2014**, *387*, 24−29.

(7) Li, X.; Wu, P.; Gao, G. F.; Cheng, S. Carbohydrate-Functionalized Chitosan Fiber for Influenza Virus Capture. *Biomacromolecules* **2011**, *12*, 3962−3969.

(8) World Health Organization. The Top 10 Causes of Death Globally. https://www.who.int/news-room/fact-sheets/detail/the-top-10-causes-of-death. (Date accessed: February 15, 2025).

(9) Nyamweya, N. N. Applications of Polymer Blends in Drug Delivery. *Future J. Pharm. Sci.* **2021**, *7*, No. 18.

(10) Wang, Y.; Chen, Y.; Du, H.; Yang, J.; Ming, K.; Song, M.; Liu, J. Comparison of the Anti-Duck Hepatitis A Virus Activities of Phosphorylated and Sulfated Astragalus Polysaccharides. *Exp. Biol. Med.* **2017**, *242*, 344−353.

(11) Talarico, L. B.; Damonte, E. B. Interference in Dengue Virus Adsorption and Uncoating by Carrageenans. *Virology* **2007**, *363*, 473−485.

(12) Yamada, T.; Ogamo, A.; Saito, T.; Uchiyama, H.; Nakagawa, Y. Preparation of O-Acylated Low-Molecular-Weight Carrageenans with Potent Anti-HIV Activity and Low Anticoagulant Effect. *Carbohydr. Polym.* **2000**, *41*, 115−120.

(13) Derby, N.; Lal, M.; Aravantinou, M.; Kizima, L.; Barnable, P.; Rodriguez, A.; Lai, M.; Wesenberg, A.; Ugaonkar, S.; Levendosky, K.; Mizenina, O.; Kleinbeck, K.; Lifson, J. D.; Peet, M. M.; Lloyd, Z.; Benson, M.; Heneine, W.; O'Keefe, B. R.; Robbiani, M.; Martinelli, E.; Grasperge, B.; Blanchard, J.; Gettie, A.; Teleshova, N.; Fernández-Romero, J. A.; Zydowsky, T. M. Griffithsin Carrageenan Fast Dissolving Inserts Prevent SHIV HSV-2 and HPV Infections in Vivo. *Nat. Commun.* **2018**, *9*, No. 3881.

(14) Wei, Q.; Fu, G.; Wang, K.; Yang, Q.; Zhao, J.; Wang, Y.; Ji, K.; Song, S. Advances in Research on Antiviral Activities of Sulfated Polysaccharides from Seaweeds. *Pharmaceuticals* **2022**, *15*, No. 581.

(15) Shi, Q.; Wang, A.; Lu, Z.; Qin, C.; Hu, J.; Yin, J. Overview on the Antiviral Activities and Mechanisms of Marine Polysaccharides from Seaweeds. *Carbohydr. Res.* **2017**, *453*−*454*, 1−9.

(16) Wang, W.; Wang, S. X.; Guan, H. S. The Antiviral Activities and Mechanisms of Marine Polysaccharides: An Overview. *Mar. Drugs* **2012**, *10*, 2795−2816.

(17) Liyanage, N. M.; Nagahawatta, D. P.; Jayawardena, T. U.; Sanjeewa, K. K. A.; Jayawrdhana, H. H. A. C. K.; Kim, J. I.; Jeon, Y. J. Sulfated Polysaccharides from Seaweeds: A Promising Strategy for Combatting Viral Diseases—A Review. *Mar. Drugs* **2023**, *21*, No. 461.

(18) Ahmadi, A.; Moghadamtousi, S. Z.; Abubakar, S.; Zandi, K. Antiviral Potential of Algae Polysaccharides Isolated from Marine Sources: A Review. *BioMed Res. Int.* **2015**, *2015*, No. 825203.

(19) Liu, H.; Zhu, Y.; Zhang, C.; Zhou, Y.; Yu, D. G. Electrospun Nanofiber as Building Blocks for High-Performance Air Filter: A Review. *Nano Today* **2024**, *55*, No. 102161.

(20) Le, B.; Omran, N.; Elnabawy, E.; Hassanin, A. H.; Mahmoud, K.; Shehata, N.; Shyha, I. Exploring Advances in Nanofiber-Based

Face Masks: A Comprehensive Review of Mechanical, Electrostatic, and Antimicrobial Functionality Filtration for the Removal of Airborne Particulate Matter and Pathogens. *Emergent Mater.* **2024**, *7*, 765−800.
(21) Habibi, S.; Ghajarieh, A. Application of Nanofibers in Virus and Bacteria Filtration. *Russ. J. Appl. Chem.* **2022**, *95*, 486−498.
(22) Pardo-Figuerez, M.; Chiva-Flor, A.; Figueroa-Lopez, K.; Prieto, C.; Lagaron, J. M. Antimicrobial Nanofiber Based Filters for High Filtration Efficiency Respirators. *Nanomaterials* **2021**, *11*, No. 900.
(23) Zhou, Y.; Liu, Y.; Zhang, M.; Feng, Z.; Yu, D. G.; Wang, K. Electrospun Nanofiber Membranes for Air Filtration: A Review. *Nanomaterials* **2022**, *12*, No. 1077.
(24) Yoshida, T. Anti-HIV Mechanism of Sulfated Poly and Oligosaccharides. *J. Fiber Sci. Technol.* **2020**, *76*, 387−402.
(25) Artan, M.; Karadeniz, F.; Karagozlu, M. Z.; Kim, M. M.; Kim, S. K. Anti-HIV-1 Activity of Low Molecular Weight Sulfated Chitooligosaccharides. *Carbohydr. Res.* **2010**, *345*, 656−662.
(26) Mourya, V. K.; Inamdar, N. N. Chitosan-Modifications and Applications: Opportunities Galore. *React. Funct. Polym.* **2008**, *68*, 1013−1051.
(27) Suryani, S.; Chaerunisaa, A. Y.; Joni, I. M.; Ruslin, R.; Anton, A.; Sartinah, A.; Ramadhan, L. O. A. N.; Aspadiah, V. The Chemical Modification to Improve Solubility of Chitosan and Its Derivatives Application, Preparation Method, Toxicity as a Nanoparticles. *Nanotechnol., Sci. Appl.* **2024**, *17*, 41−57.
(28) Edo, G. I.; Yousif, E.; Al-Mashhadani, M. H. Modified Chitosan: Insight on Biomedical and Industrial Applications. *Int. J. Biol. Macromol.* **2024**, *275*, No. 133526.
(29) Milewska, A.; Chi, Y.; Szczepanski, A.; Barreto-Duran, E.; Dabrowska, A.; Botwina, P.; Obloza, M.; Liu, K.; Liu, D.; Guo, X.; Ge, Y.; Li, J.; Cui, L.; Ochman, M.; Urlik, M.; Rodziewicz-Motowidlo, S.; Zhu, F.; Szczubialka, K.; Nowakowska, M.; Pyrc, K. HTCC as a Polymeric Inhibitor of SARS-CoV-2 and MERS-CoV. *J. Virol.* **2021**, *95*, No. 10-1128.
(30) Milewska, A.; Kaminski, K.; Ciejka, J.; Kosowicz, K.; Zeglen, S.; Wojarski, J.; Nowakowska, M.; Szczubiałka, K.; Pyrc, K. HTCC: Broad range Inhibitor of coronavirus entry. *PLoS One* **2016**, *11*, No. e0156552.
(31) Dhlamini, K. S.; Selepe, C. T.; Ramalapa, B.; Cele, Z.; Malatji, K.; Govender, K. K.; Tshweu, L.; Ray, S. S. Dual Antimicrobial Activity of HTCC and Its Nanoparticles: A Synergistic Approach for Antibacterial and Antiviral Applications Through Combined In Silico and In Vitro Studies. *Polymers* **2024**, *16*, No. 2999.
(32) Yan, C.; Chen, D.; Gu, J.; Hu, H.; Zhao, X.; Qiao, M. Preparation of N-Succinyl-Chitosan and Their Physical-Chemical Properties as a Novel Excipient. *Yakugaku Zasshi* **2006**, *126*, 789−793.
(33) Hoque, J.; Adhikary, U.; Yadav, V.; Samaddar, S.; Konai, M. M.; Prakash, R. G.; Paramanandham, K.; Shome, B. R.; Sanyal, K.; Haldar, J. Chitosan Derivatives Active against Multidrug-Resistant Bacteria and Pathogenic Fungi: In Vivo Evaluation as Topical Antimicrobials. *Mol. Pharmaceutics* **2016**, *13*, 3578−3589.
(34) Kaihara, S.; Suzuki, Y.; Fujimoto, K. In Situ Synthesis of Polysaccharide Nanoparticles via Polyion Complex of Carboxymethyl Cellulose and Chitosan. *Colloids Surf., B* **2011**, *85*, 343−348.
(35) Wei, X.; Decker, J. M.; Wang, S.; Hui, H.; Kappes, J. C.; Wu, X.; Salazar-Gonzalez, J. F.; Salazar, M. G.; Kilby, J. M.; Saag, M. S.; Komarova, N. L.; Nowak, M. A.; Hahn, B. H.; Kwong, P. D.; Shaw, G. M. Antibody Neutralization and Escape by HIV-1. *Nature* **2003**, *422*, 307−312.
(36) Fonseca-Santos, B.; Chorilli, M. An Overview of Carboxymethyl Derivatives of Chitosan: Their Use as Biomaterials and Drug Delivery Systems. *Mater. Sci. Eng., C* **2017**, *77*, 1349−1362.
(37) Kerwald, J.; de Moura Junior, C. F.; Freitas, E. D.; Ochi, D.; Sorrechia, R.; Pietro, R. C. L. R.; Beppu, M. M. Coating of Surgical Masks with Quaternized Chitosan Aiming at Inactivating Coronavirus and Antibacterial Activity. *Carbohydr. Polym. Technol. Appl.* **2023**, *5*, No. 100315.
(38) Feketefoldi, B.; Cermenek, B. Chitosan-Based Anion Exchange Membranes for Direct Ethanol Fuel Cells. *J. Membr. Sci. Technol.* **2016**, *06*, 2155−9589.
(39) Zhang, S.; Huang, S.; Lu, L.; Song, X.; Li, P.; Wang, F. Curdlan Sulfate-O-Linked Quaternized Chitosan Nanoparticles: Potential Adjuvants to Improve the Immunogenicity of Exogenous Antigens via Intranasal Vaccination. *Int. J. Nanomed.* **2018**, *13*, 2377−2394.
(40) Xi, X.; Zhen, W.; Bian, S. Preparation and Properties of Polylactic Acid/N-(2-Hydroxyl) Propyl-3-Trimethyl Ammonium Chitosan Chloride-Intercalated Saponite Nanocomposites. *Iran. Polym. J.* **2015**, *24*, 243−252.
(41) Maiz-Fernández, S.; Pérez-Álvarez, L.; Silván, U.; Vilas-Vilela, J. L.; Lanceros-Méndez, S. Dynamic and Self-Healable Chitosan/Hyaluronic Acid-Based In Situ-Forming Hydrogels. *Gels* **2022**, *8*, No. 477.
(42) Cabral, J. D.; Roxburgh, M.; Shi, Z.; Liu, L.; McConnell, M.; Williams, G.; Evans, N.; Hanton, L. R.; Simpson, J.; Moratti, S. C.; Robinson, B. H.; Wormald, P. J.; Robinson, S. Synthesis, Physiochemical Characterization, and Biocompatibility of a Chitosan/Dextran-Based Hydrogel for Postsurgical Adhesion Prevention. *J. Mater. Sci.: Mater. Med.* **2014**, *25*, 2743−2756.
(43) Li, X.; Wang, Y.; Li, A.; Ye, Y.; Peng, S.; Deng, M.; Jiang, B. A Novel PH- And Salt-Responsive n-Succinyl-Chitosan Hydrogel via a One-Step Hydrothermal Process. *Molecules* **2019**, *24*, No. 4211.
(44) Ciro, Y.; Rojas, J.; Alhajj, M. J.; Carabali, G. A.; Salamanca, C. H. Production and Characterization of Chitosan−Polyanion Nanoparticles by Polyelectrolyte Complexation Assisted by High-Intensity Sonication for the Modified Release of Methotrexate. *Pharmaceuticals* **2020**, *13*, No. 11.
(45) Briggs, J. A. G.; Wilk, T.; Welker, R.; Kräusslich, H. G.; Fuller, S. D. Structural Organization of Authentic, Mature HIV-1 Virions and Cores. *EMBO J.* **2003**, *22*, 1707−1715.
(46) Filippov, S. K.; Khusnutdinov, R.; Murmiliuk, A.; Inam, W.; Zakharova, L. Y.; Zhang, H.; Khutoryanskiy, V. V. Dynamic Light Scattering and Transmission Electron Microscopy in Drug Delivery: A Roadmap for Correct Characterization of Nanoparticles and Interpretation of Results. *Mater. Horiz.* **2023**, *10*, 5354−5370.
(47) Borrego, M.; Martín-Alfonso, J. E.; Valencia, C.; Sánchez Carrillo, M. D. C.; Franco, J. M. Developing Electrospun Ethylcellulose Nanofibrous Webs: An Alternative Approach for Structuring Castor Oil. *ACS Appl. Polym. Mater.* **2022**, *4*, 7217−7227.
(48) Qosim, N.; Majd, H.; Ahmed, J.; Williams, G.; Edirisinghe, M. Making Fibers from Cellulose Derivatives by Pressurized Gyration and Electrospinning. *Cellulose* **2024**, *31*, 2815−2832.
(49) Shenoy, S. L.; Bates, W. D.; Frisch, H. L.; Wnek, G. E. Role of Chain Entanglements on Fiber Formation during Electrospinning of Polymer Solutions: Good Solvent, Non-Specific Polymer-Polymer Interaction Limit. *Polymer* **2005**, *46*, 3372−3384.
(50) Nugraha, A. S.; Chou, C. C.; Yu, P. H.; Lin, K.-L. Effects of applied voltage on the morphology and phases of electrospun poly(vinylidene difluoride) nanofibers. *Polym. Int.* **2022**, *71*, 1176−1183.
(51) Zienkiewicz-Strzałka, M.; Deryło-Marczewska, A.; Skorik, Y. A.; Petrova, V. A.; Choma, A.; Komaniecka, I. Silver Nanoparticles on Chitosan/Silica Nanofibers: Characterization and Antibacterial Activity. *Int. J. Mol. Sci.* **2020**, *21*, No. 166.
(52) Wu, J. Y.; Wang, C. Y.; Chen, K. H.; Lai, Y. R.; Chiu, C. Y.; Lee, H. C.; Chang, Y. K. Electrospinning of Quaternized Chitosan-Poly(Vinyl Alcohol) Composite Nanofiber Membrane: Processing Optimization and Antibacterial Efficacy. *Membranes* **2022**, *12*, No. 332.
(53) Nordi, S. S.; Noor, E. E. M.; Kok, C. K.; Julkapli, N. M.; Baig, M. F. Phase, Chemical, Thermal, and Morphological Analyses of Thermoplastic Polyurethane (TPU) Nanocomposites Reinforced with Jute Cellulose Nanofibers (CNFs). *Polymers* **2025**, *17*, No. 899.
(54) Alekseeva, O. V.; Noskov, A. V.; Agafonov, A. V. Structure, Physicochemical Properties, and Adsorption Performance of the Ethyl Cellulose/Bentonite Composite Films. *Cellulose* **2022**, *29*, 3947−3961.

https://doi.org/10.1021/acsanm.5c03567
ACS Appl. Nano Mater. XXXX, XXX, XXX−XXX

(55) Ottenhall, A.; Henschen, J.; Illergård, J.; Ek, M. Cellulose-Based Water Purification Using Paper Filters Modified with Polyelectrolyte Multilayers to Remove Bacteria from Water through Electrostatic Interactions. *Environ. Sci.* **2018**, *4*, 2070−2079.
(56) Ghiasi, S.; Behboudi, A.; Mohammadi, T.; Khanlari, S. Effect of Surface Charge and Roughness on Ultrafiltration Membranes Performance and Polyelectrolyte Nanofiltration Layer Assembly. *Colloids Surf., A* **2019**, *580*, No. 123753.
(57) Hao, Q.; Schossig, J.; Davide, T.; Towolawi, A.; Zhang, C.; Lu, P. Gravity-Driven Ultrahigh-Speed Electrospinning for the Production of Ethyl Cellulose Fibers with Tunable Porosity for Oil Absorption. *ACS Sustainable Chem. Eng.* **2025**, *13*, 507−517.
(58) Chen, Y.; Wang, Y.; Wan, J.; Ma, Y. Crystal and Pore Structure of Wheat Straw Cellulose Fiber during Recycling. *Cellulose* **2010**, *17*, 329−338.
(59) Smart Water Magazine. What Is the Difference between Microfiltration, Ultrafiltration and Nanofiltration? *Smart Water Mag.* 2019, pp 1−8.
(60) Chen, Y.; Tan, G. Z.; Zhou, Y. Effects of Viscosities and Solution Composition on Core-Sheath Electrospun Polycaprolactone-(PCL) Nanoporous Microtubes. *Polymers* **2021**, *13*, No. 3650.
(61) Wu, D.; Ensinas, A.; Verrier, B.; Primard, C.; Cuvillier, A.; Champier, G.; Paul, S.; Delair, T. Zinc-Stabilized Chitosan-Chondroitin Sulfate Nanocomplexes for HIV-1 Infection Inhibition Application. *Mol. Pharmaceutics* **2016**, *13*, 3279−3291.
(62) Cele, Z. E. D.; Matshe, W.; Mdlalose, L.; Setshedi, K.; Malatji, K.; Mkhwanazi, N. P.; Ntombela, T.; Balogun, M. Cationic Chitosan Derivatives for the Inactivation of HIV-1 and SARS-CoV-2 Enveloped Viruses. *ACS Omega* **2023**, *8*, 31714−31724.
(63) Sosa, M. A. G.; Fazely, F.; Koch, J. A.; Vercellotti, S. V.; Ruprecht, R. M. N-Carboxymethylchitosan-N,O-Sulfate as an Anti-HIV-1 Agent. *Biochem. Biophys. Res. Commun.* **1991**, *174*, 489−496.
(64) Wasilewska, K.; Winnicka, K. Ethylcellulose-a Pharmaceutical Excipient with Multidirectional Application in Drug Dosage Forms Development. *Materials* **2019**, *12*, No. 3386.
(65) Krasian, T.; Daranarong, D.; Punyodom, W.; Manokruang, K.; Somsunan, R.; Jantrawut, P.; Chaiwarit, T.; Panraksa, P.; Jantanasakulwong, K.; Rachtanapun, P.; Worajittiphon, P. Electrospun Composite Membranes of Ethyl Cellulose and MXene (Ti3C2Tx): Biocompatible Platforms for Enhanced Drug Delivery and Antibacterial Wound Healing. *Int. J. Biol. Macromol.* **2025**, *287*, No. 138596.
(66) Hadzhieva, Z.; Bider, F.; Kissel, H.; Damian-Buda, A.-I.; Boccaccini, A. R. Electrospun cellulose filters with antiviral properties: review of developments in the last 5 years. *Chem. Eng. J. Adv.* **2025**, *23*, No. 100776.
(67) Akin, E.; Gharibzahedi, S. M. T.; Qiu, H.; Aliyeva, A.; Altintas, Z. Chitosan-Functionalized PVDF and PES Membranes Integrated by Epitope-Imprinted Polymers for Targeted Hepatitis A Virus Capture. *J. Membr. Sci.* **2024**, *709*, No. 123084.
(68) Wu, J. Y.; Ooi, C. W.; Song, C. P.; Wang, C. Y.; Liu, B. L.; Lin, G. Y.; Chiu, C. Y.; Chang, Y. K. Antibacterial Efficacy of Quaternized Chitosan/Poly (Vinyl Alcohol) Nanofiber Membrane Crosslinked with Blocked Diisocyanate. *Carbohydr. Polym.* **2021**, *262*, No. 117910.
(69) Cheah, W. Y.; Show, P. L.; Ng, I. S.; Lin, G. Y.; Chiu, C. Y.; Chang, Y. K. Antibacterial Activity of Quaternized Chitosan Modified Nanofiber Membrane. *Int. J. Biol. Macromol.* **2019**, *126*, 569−577.

https://doi.org/10.1021/acsanm.5c03567
ACS Appl. Nano Mater. XXXX, XXX, XXX−XXX